Plant-mediated Synthesis of Silver Nanoparticles Using Leaf extract of *Salvadora oleoides* Decne.: Green nanofertilizer from *Salvadora oleoides* Decne

Rutvik Thakkar[1], Snehal Patel[2*], and N.K. Patel[3]

[123]Department of Botany, Sheth M.N. Science College, Patan-384265, Gujarat, India

Received: Jun 5, 2025 **Accepted:** Jul 3, 2025 **Published:** Jul 5, 2025

Abstract

In this study, *Salvadora oleoides* leaf extract was used to create silver nanoparticles (AgNPs) in a quick, affordable, and ecologically friendly manner. There were several methodologies employed to characterize the synthesised AgNPs. A prominent SPR peak at 431 nm was detected by UV-Vis spectrophotometry, proving that silver nanoparticles were successfully formed. The shape of the nanoparticles was investigated utilizing SEM and TEM, and elemental silver was discovered. The fcc structure of metallic silver was confirmed by purity and crystal structure investigation utilizing XRD, which revealed the presence of the (111), (200), (220), and (311) lattice planes. Both the capping agents contained in the leaf extract and those particular functional groups that are accountable for transforming silver nitrate to AgNPs were identified using FTIR. Silver nanoparticles with sizes ranging from 18 to 32 nm are visible in images taken using Scanning electron microscope and transmission electron microscopy. Furthermore, the seed germination of the silver nanoparticles from *S. oleoides* was investigated utilizing tomato seeds. Concentration taken was 0.3%, 0.5%, 0.8%, 1%, 3%, 5%, 10%, 20%, 25%, 50% and 100% of AgNPs solution. These findings point to prospective applications in a variety of sectors, such as agriculture and healthcare.

Keywords: - *Salvadora oleoides, AgNPs, Leaf extract, Seed germination*

1. Introduction

Due to its many applications, nanotechnology is currently becoming more well known and is expected to advance. Electronics, biological sciences, medicines, cosmetics preparations, water filtration, and catalytic systems are only a few of the many uses in the technology sector [1]. The standards of physical and synthetic methods are combined in nanotechnology to shape nanosized particles with a clear limit. Nanotechnology has been more and more valued in the life sciences during the past few decades, especially in the domains of biomedical devices and medicine.

Depending on unusual characteristics like size, shape, and elaboration, nanoparticles exhibit entirely new or better resources [2]. The fundamental units of nanotechnology are nanoparticles. Additionally, nanoparticles (NPs) of reputable metals like silver and gold have anticipated uses in a variety of industries, including biomedicine, where they can be applied to the development of high-quality drug delivery systems and the treatment of certain tumours [3]. Different sources of gas, liquid, or solid-stage nanoparticles are available. Along with chemical synthesis, thermal degradation, and electrochemical, photochemical, and organic synthesis, there are several methods for creating silver nanoparticles. Environmentally hazardous, expensive, and requiring a lot of energy, chemical and physical approaches for creating nanoparticles is not recommended [4].

One such significant individual from the noble metal NPs is silver (Ag NPs), generally utilized in shampoos, soaps, cosmetics, toothpaste, medicinal and pharmaceutical items [5, 6]. AgNPs have been described and studied thoroughly with the entirety of their properties noteworthy to modern-day science and prevailing technologies. Silver nanoparticles have pulled in more consideration for their captivating electrical, thermal, and optical properties. Silver has the most noteworthy electrical conductivity (6.3×10^{-7} S/m) in the midst of the considerable number of metals, by underneath that silver Nanoparticles are taken into consideration as a very extremely confident applicant in flexible electronics [7-9]. The significant preferred position of utilizing plant extracts for AgNPs synthesis is that they are effectively procurable, reliable, and nontoxic in most cases, have an expansive decent variety of metabolites that can assist in the reduction of silver ions, and are quicker than microbes within the synthesis. The essential instrument considered for the cycle is plant-assisted reduction due to phytochemicals. Flavones, natural acids, and quinones are water-dissolvable phytochemicals that are liable for the prompt decrease of the ions. Studies have disclosed that xerophytes incorporate emodin, an anthraquinone that goes through tautomerization, striking to the progress of the AgNPs. It absolutely was steered that the phytochemicals are involved overtly within the reduction of the ions and formation of AgNPs [10].

Salvadora oleoides Decne. is an evergreen tree and shrub and belongs to the family Salvadoraceae. It is commonly known as piludi. It mainly grows in arid and alkaline soil condition and is distributed in the dry and saline desert areas [11]. The leaves are used as cooling agents and blood purifier. *S. oleoides* extracts are testified to hold various pharmaco logical activities like antimicrobial [12], anti-inflammatory [13], antiplasmodial [14], etc.

Due to above said reasons in the in-attendance study synthesized Ag nanoparticles utilizing aqueous extracts of fresh leaves of *S. oleoides* and afterward assessed its antibacterial activity against some pathogenic bacteria.

2. Materials and Methods

2.1 Collection of plant material and Seed

Salvadora oleoides fresh leaves were collected from native places of patan and tomato seeds were also collected from local vendor in patan, Gujarat, India (Location: 23°51’35”N 72°07’56”E).

2.2 Preparation of aqueous leaf extract

The aqueous extract of the sample was prepared threw utilizing the freshly accumulated 5g leaves, washing in running faucet water, and afterward in double-distilled water. Followed by heating up the slashed leaves with 100 ml of refined water, at 60°C for 5 minutes [15]. The mixture was sifted utilizing the Whatman 1 filter paper and afterward centrifuged for 20 minutes at 10000 rpm. The extract was stored in a refrigerator at 4°C for additional utilization.

2.3 Synthesis of Silver nanoparticles

In order to create Ag nanoparticles, a 1mM liquid suspension of silver nitrate ($AgNo_3$) was created. For the reduction of Ag0 to Ag+ ions, 50 ml of aqueous solution containing 1 mM silver nitrate ($AgNo_3$) was added along with 50 ml of *S. oleoides* leaf extract [16]. Through colour perception, the visual evaluation of embedded silver nanoparticles was captured. Centrifugation was used to collect the AgNPs for 15 min. at 10,000 rpm. For the purpose of getting away of the unaltered metallic ions, distilled water was used to wash the obtained pellet. For further use in spectrum analysis and antibacterial activity, the assortment was kept in the refrigerator.

2.4 Characterizations of AgNPs

Utilizing a UV-visible spectrophotometer (Lambda 750 from Perkin Elmer, USA), the UV-Vis spectra of silver NPs reaction mixture aliquots were observed dependent on SPR as a function of response time inside 300-600 nm frequencies at a resolution of 1 nm. To examine the crystallographic structure of the purified AgNPs, X-ray diffractometer (XRD) data for

drop covered, air-dried samples on glass substrate were recorded at 40 kV, 15 mA with 2h scans from 20° to 80° at 0.04° per min with a period consistent of 2s by an Ultima IV X-ray powder diffractometer (Panalytical's X'Pert Pro). Using a Perkin Elmer instrument (Norwalk, CT, USA), FTIR spectra of plant extract and AgNPs were obtained over the 3800-600 cm-1 region from 24 scans with a resolution of 2 cm-1. To examine the characteristics (form and size) of AgNPs, JEOL JXA-8230 was used for SEM. TEM is analogous to the optical microscope. It provides very high resolution which can reach approximately 0.1 nm in the case of lattice images. Consequently, very high magnification (Close to 1 million times) can be obtained.

2.5 Seeds preparation

The seeds were treated with 1.0 % sodium hypochlorite solution (NaOCl, SigmaAldrich, India) for 3 min for surface sterilization to re move fungal spores and again washed thoroughly with distilled water under aseptic conditions before being used in the experiments. All seeds were subsequently transferred into Petri dishes containing one piece of filter paper (90 mm in diameter, Whatman No.1). 15 seeds were evenly spaced on top of the filter paper in each Petri dish and 5 mL of different silver nanoparticle suspensions and control (distilled water) were added. Lastly, the plates were covered and left to germinate the seeds at room temperature (30 ± 5 ℃) on a lab bench. Three duplicates of the experiment were conducted. By dividing the total number of seeds in each dish by the number of seeds that produced a primary root of at least 3 mm, the germination percentages were calculated. After seven days, the number of seeds that had germinated in each dish was counted, and the germination percentage was computed using the formula below.

Germination (%) = The number of germinated seeds/numbers of experimental seeds×100

2.6 Statistical Analysis

Each treatment was conducted with three replicates and total mean length of primary root, shoot and seedlings were measured after 5 days of inoculation and recorded data was analysed using SPSS as mean values ± SE. Each experimental value was compared to its corresponding control.

3. Result and Discussion

3.1 UV–Vis spectra analysis

The UV–visible spectroscopy method is used to identify the characteristic SPR pattern of metal nanoparticles. The formation of AgNPs was initially verified by optical perception when the colour of the reaction mixture turned brown. After mixing the silver nitrate solution (AgNo3) (B) with the yellow aqueous leaf extract (A), they were heated to 60°C for ten minutes. The colour change to brown (C) (Fig 1) verified the emergence of Ag nanoparticles. Numerous biomolecules in the leaf extract reduced Ag+ to Ag0, which caused this colour shift. At 30-minute, 1-hour, 3-hour, and 24-hour intervals, the Uv-vis spectra acquired from the start of response in *S. oleoides* are shown in Figure 2. The colour intensity rose in tandem with the response time. AgNPs' Uv-vis absorption band value, which is an incentive in the visible light region (420-450 nm), confirms the presence of SPR. The emergence of Ag nanoparticles was periodically observed using UV-Vis spectroscopy. A leaf of *S. oleoides* showed a striking peak of silver nanoparticles at about 431 nm, as seen in Fig. 3.

The SPR peak in *A. nervosa* began to show up in the visible range at 419 nm after 30 minutes, and it gradually gained prominence. The SPR peak intensified as the reaction time increased, signifying the creation of metallic silver nanoparticles. The production of silver nanoparticles from *A. nervosa* leaves yielded an SPR peak at about 435 nm [17], while the leaf portion of *V. negundo* showed a peak value at 423 nm [18], which was comparable to the current investigation.

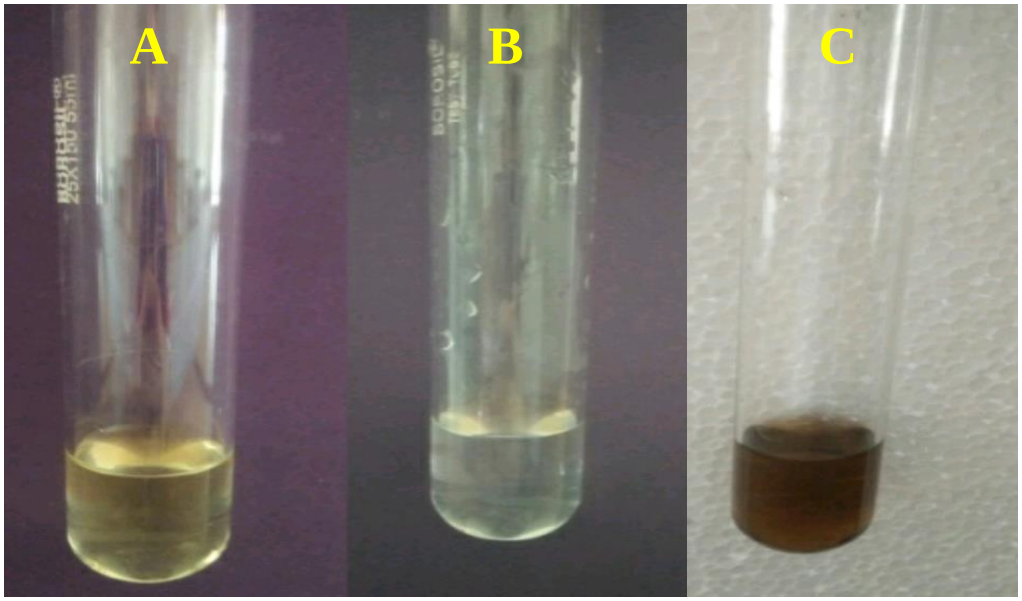


Fig 1: Optical observation (A) *S. oleoides* Leaf extracts (B) $AgNo_3$ solution (C) Synthesized AgNPs

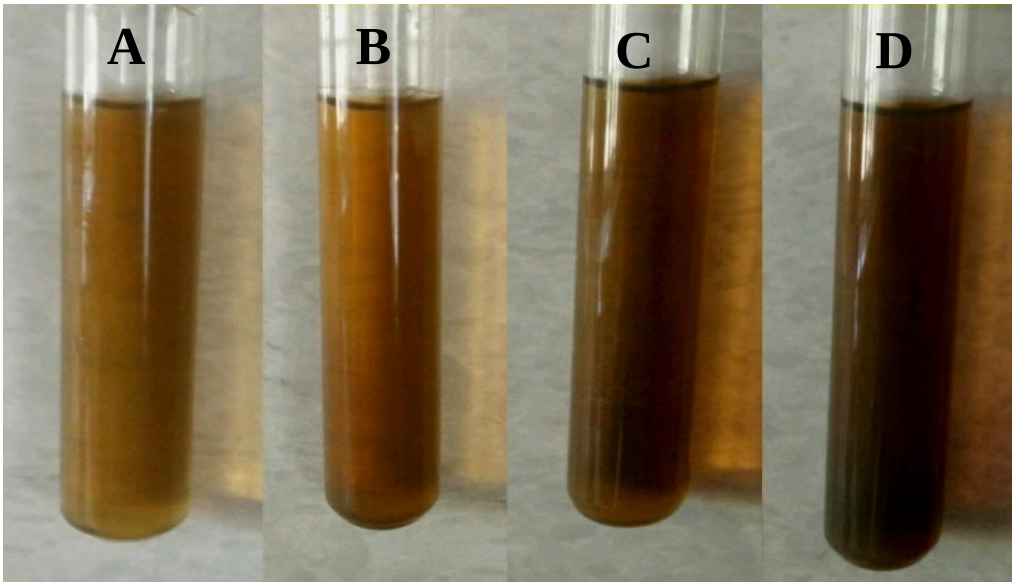


Fig 2: Showing different time interval colour intensity of *S. oleoides* leaf extract with AgNPs (A) After 30 mins (B) After 1 hr (C) After 3 hrs (D) After 24 hrs

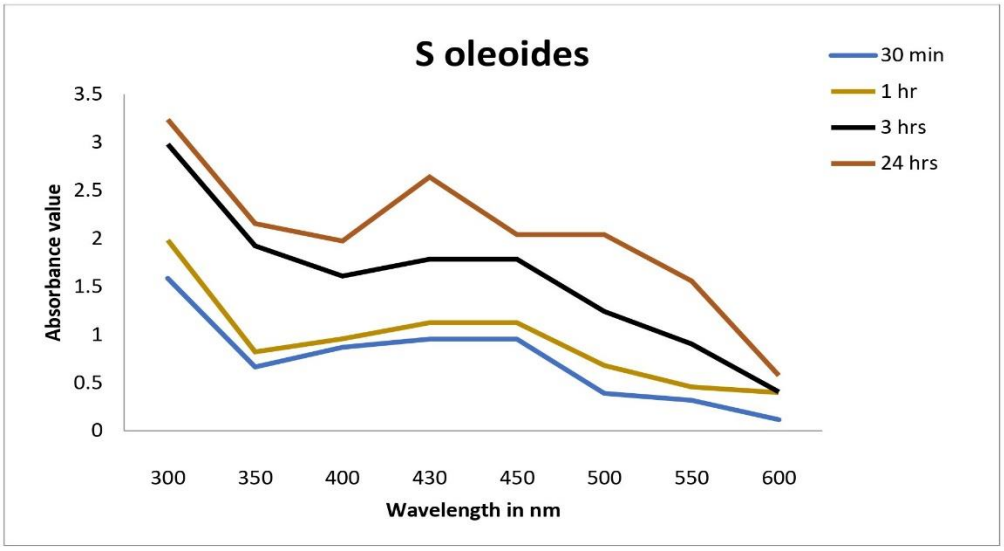


Fig 3: UV-visible spectra of *S. oleoides* AgNPs obtained using leaf extract of *S. oleoides* at different time intervals

3.2 X-Ray diffraction Analysis

XRD for drop coated air-dried samples on glass substrate used to be recorded with 2θ scans from 20° to 80° at 0.04° per min with a time steady of 2s by X-ray diffractometer (XRD) to study the crystallographic structure of the purified *S. oleoides* AgNPs. The crystalline nature of the *S. oleoides* AgNPs used to be decided by way of powder XRD, as shown in Fig. 4. Bragg's reflections were detected at 2θ= 38.15°, 44.42°, 64.50°, and 77.37°, which correspond to the face-centered cubic (fcc) structures' (111), (200), (220), and (311) planes, respectively. The XRD examination of AgNPs was used to derive a number of parameters, as shown in Table 1. Scherrer's formula, D=kλ/β cosθ, is used to calculate the average crystal size of the silver nanoparticles created during the bioreduction process. This formula also displays the XRD pattern of the silver nanoparticles formed in *S. oleoides*. where ß is the full width at half maximum (FWHM) of the diffraction peak in radians, D is the AgNPs crystallite size, k is the Scherrer constant, which ranges from 0.9 to 1, and h is the Bragg angle in radians used in XRD. The average crystallite size was calculated to be 21 nm. This is in accordance with JCPDS No. 04-0873, the typical metallic silver XRD pattern. Additionally, XRD revealed a couple exceptionally strong peaks that were left unidentified in Figure 4. The crystallization of the bioorganic phase on the AgNPs' surface is thought to be the cause of these extra peaks. Indeed, the SEM makes this quite evident, and the FT-IR and UV investigations confirm it as well.

Similarly, other research on the synthesis of AgNPs using other extracts also showed additional peaks. The diffractogram of AgNPs made from *Azadirachta indica* leaf extract, for example, shows multiple extra peaks [19]. Similar studies have been conducted on other plants, such as *Capparis Zeylanica* leaf extract, where the XRD pattern was utilized to verify that the produced AgNPs were found to be extremely stable and crystalline [20].

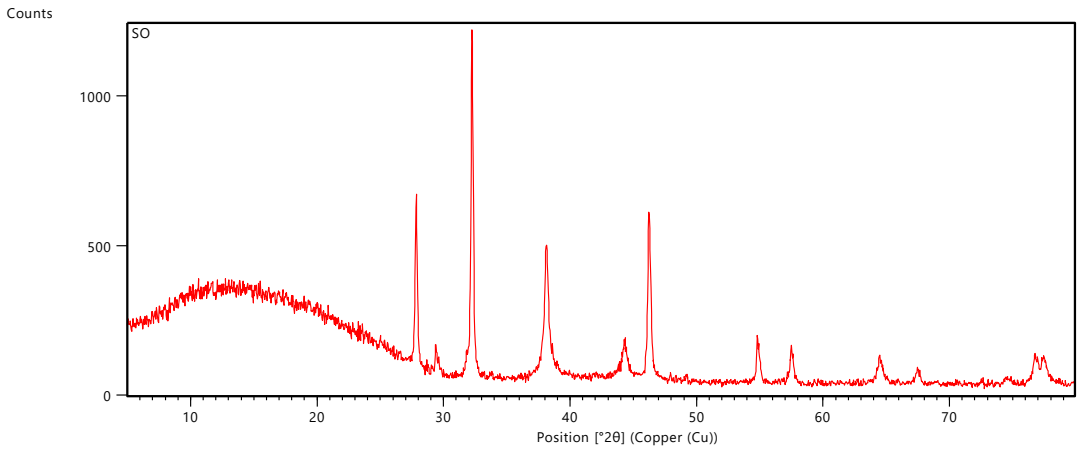


Fig 4: XRD pattern of AgNPs synthesized using the leaves extract of *S. oleoides*

2Ɵ (Degree)	FWHM	Diffraction plane (hk1)	Interplanar spacing "d"	Crystallite size (nm)
38.15°	0.51	111	0.83	19.45
44.42°	0.74	200	0.97	23.50
64.50°	0.57	220	0.92	21.21
77.37°	0.70	311	1.20	18.20

Table 1: Different parameters of the XRD analysis of AgNPs of *S. oleoides* leaf extract

3.3 Fourier Transform Infrared (FTIR) Spectroscopy Analysis

Chemical components involved in the synthesis of AgNPs are characterized using FT-IR spectroscopy. Plant extract and AgNPs were used in powdered form for the study in order to identify the various functional groups responsible for the reduction of silver nitrate to silver nanoparticles. AgNPs' and plant extract's spectra (Fig. 5) were generally comparable. As illustrated in Figure 5, the FTIR spectrum displayed a number of noteworthy peaks. To identify the biomolecules for capping and effective stability of the produced metallic nanoparticles, FTIR studies were performed. Biosynthesized silver nanoparticles exhibit a band at 3996, 3460, 2760, 2661, 2137, 1369, 1128, 657, and 597 cm-1 in their FTIR spectra. O-H stretching for alcohols, single aldehyde stretching (2760 cm-1), C-H stretching (2661 cm-1), -C≡C stretching for Alkeynes (2137 cm-1), C=C stretching for aromatic rings (1369 cm-1), and C-Cl and C-Br stretching in alkyl groups (597 cm-1 and 657 cm-1).

The FTIR analysis results indicate that the peaks near 3440cm−1, 2924cm−1, and 2854cm−1 are attributed to OH stretching and aldehydic C–H stretching, respectively; 3432.94—N–H stretch, 2777.28—single aldehyde, 2676.19—C–H; O–H, 2071.75—C≡C, 1637.58—C=C, and 1121.56—C=O [21]. Absorption bands at 3419, 1749, 2927, 1625, 1383, 1235, 1069, 832, and 602 cm-1 were visible in the spectra. The phenolic chemicals in the *phlomis* leaf extract caused –OH stretching, which was shown by the prominent peaks at 3419 cm-1 [22].

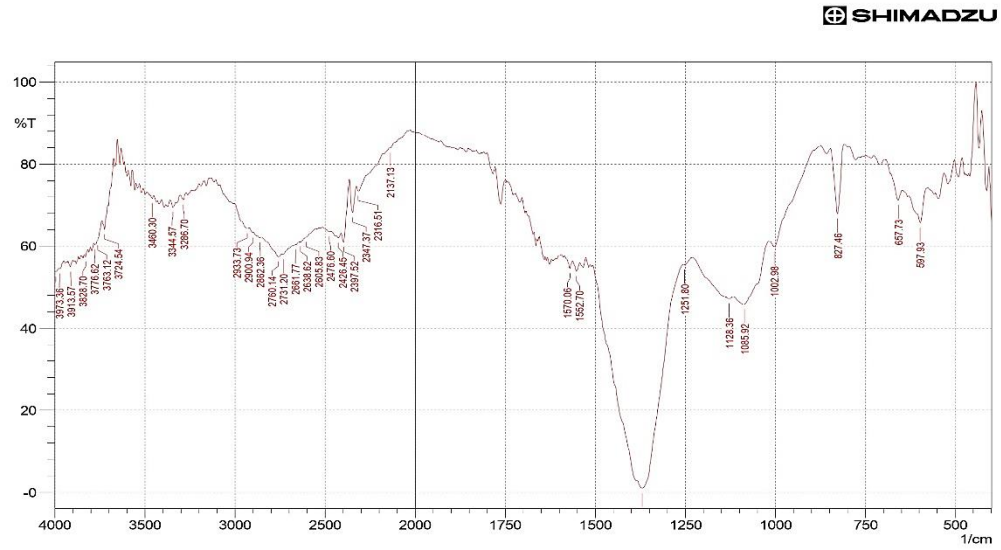


Fig 5: FTIR spectra of synthesized AgNPs of *S. oleoides*

3.4 SEM Analysis

Scanning electron microscopy was used to examine the AgNPs' surface shape. Figure 6 confirmed well-characterized spherical AgNPs without agglomeration. In SEM analysis, the material is experimented with in a sequence of parallel tracks using an electron film beam (10 KeV). By interacting with an electron in the sample, these electrons produce a variety of detectable indications that also contain sample data. The structure of the generated reaction products was determined by SEM analysis. The morphology of the AgNPs integrated during green synthesis was examined using a SEM. Figure 6 displays the SEM pictures taken at 300 nm (A) and 500 nm (B). Furthermore, the image obtained from the SEM image shows that the average size of silver nanoparticles is 20–25 nm. The SEM measurement of the Ag NPs' size (21 nm) agrees with the XRD analysis. The creation of silver nanoparticles was clearly demonstrated by the SEM examinations, which confirmed the formation of silver particles in the 20–30 nm size range.

A similar outcome was obtained using Elettaria cardamom seed extract; the SEM result revealed that the resulting nanoparticle had a spherical shape and ranged in size from 40 to 70 nm [23]. The SEM result for an extract of Viburnum lantana leaves indicates that they are spherical in shape and range in size from 20 to 80 nm [24].

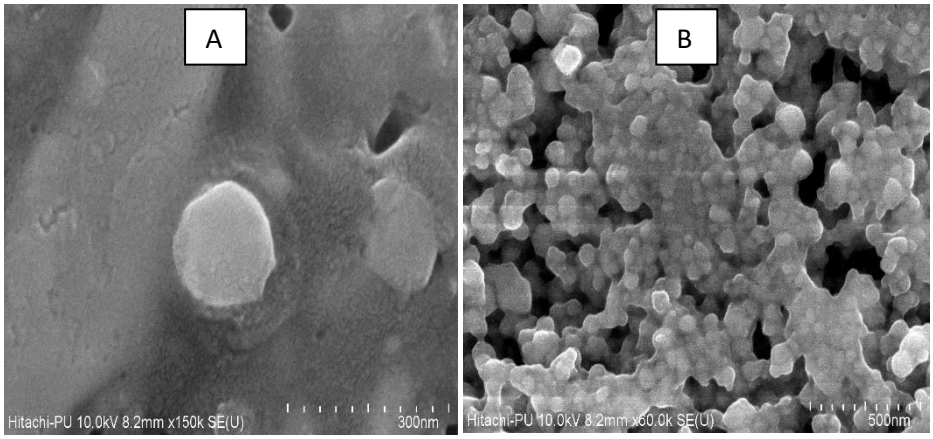


Fig 6: Scanning electron microscopy (SEM) images of AgNPs by *S. oleoides* (A) 300 nm (B) 500 nm

3.5 TEM Analysis

The size, shape, and morphology of nanoparticles have been ascertained by the use of transmission electron microscopy. It illustrates that the silver nanoparticles are mostly spherical and widely dispersed, while some were found to have irregular shapes, as seen in Fig. 7. The form of the SPR band in the UV-visible spectrum indicates that the nanoparticles are spherical and homogenous. With an average diameter of about 7 nm and a variable nano range of 100, 20, 10, and 5 nm, the particle size matches that seen in the histogram (Fig 7). Figures also show variations in particle size and size distribution. The measured particle size ranges from 18 to 32 nm, with an average of 25 nm.

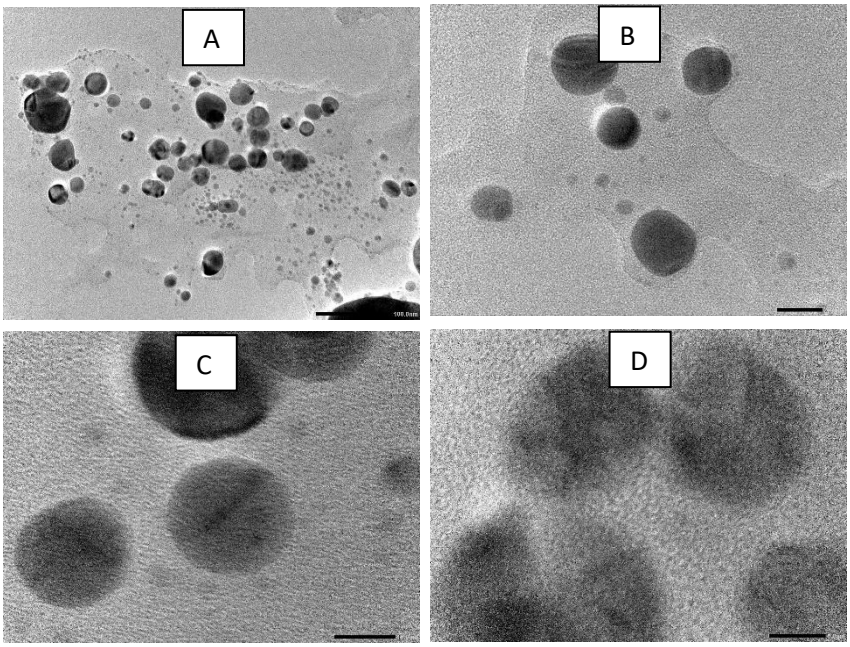


Fig 7: Transmission electron microscopy (TEM) images of AgNPs by *S. oleoides* (A) 100 nm (B) 20 nm (C) 10 nm (D) 5 nm

3.6 Seed germination activity

For up to seven days, different quantities of nano biofertilizer 0.3%, 0.5%, 0.8%, 1%, 3%, 5%, 10%, 20%, 25%, 50% and 100% of AgNPs were sprayed every two days. Plants treated with 0.3 % concentration had greater seed germination than those treated with 0.5%, 0.8%, 1%, 3%, 5%, 10%, 20%, 25%, 50% and 100%, and control (Fig. 8). As per fig 8, tomato seed shows the better result in lesser concentration of silver NPs and by increasing the concentration it shows lesser seed germination. Fig 8 shows some photos of seed germination activity. Tomatoes are high in proteins, carbohydrates, sodium, potassium, and phosphorus, which may account for their enhanced fresh weight and vigor when treated with nano biofertilizer. The growth and development of plants are greatly influenced by these mineral nutrients. Potassium citrate boosts productivity, improves fruit quality, increases leaf area, and increases leaf mineral content [25]. In a similar vein, when compared to the control tomato, the application of nano silver liquid displayed the highest fresh and dry weights [26].

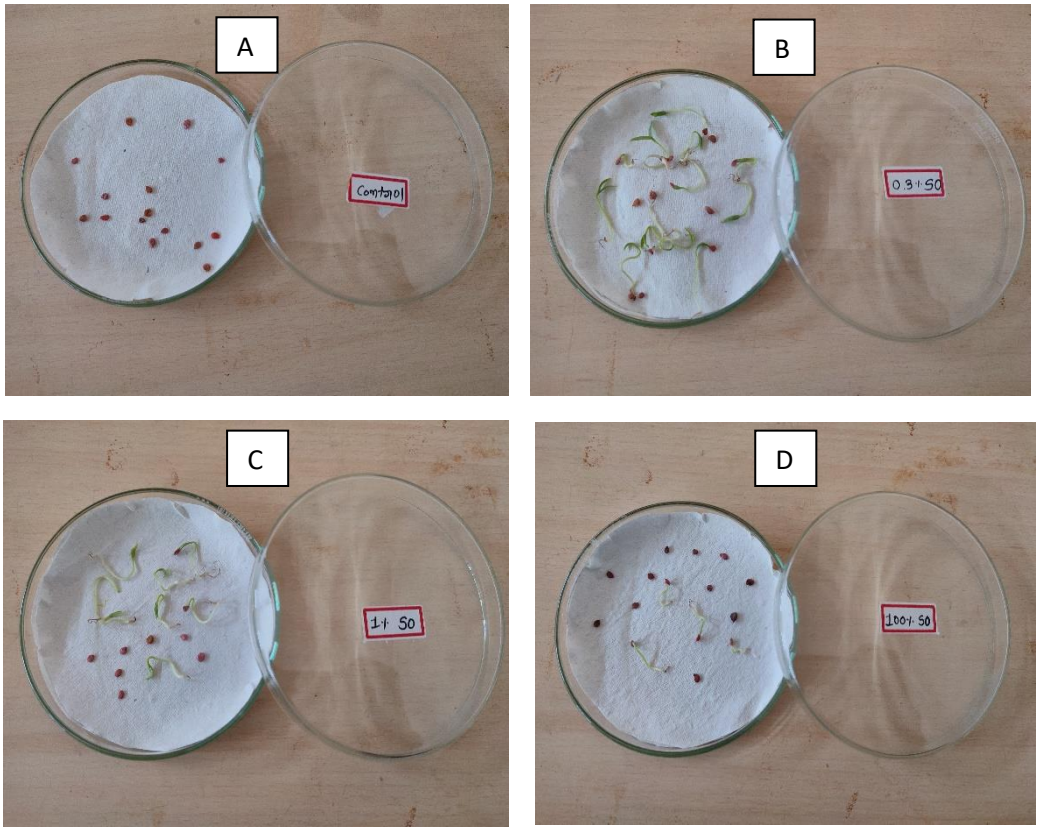


Fig 8: Seed germination activity of *S. oleoides* (A) control (B) 0.3 % solvent (C) 1% solvent (D) 100% solvent

Conclusion

Silver nanoparticles were successfully synthesized via a plant-mediated, environmentally friendly process that made use of *S. oleoides* leaf extract. It was discovered that the different biomolecules detected in the leaf extract were in charge of the NPs' stability and production. UV-Vis spectroscopy, XRD, FTIR, and SEM were used to illustrate the size, shape, crystalline structure, and stability. The NPs' fcc structure, average size of 20–25 nm, and presence of functional groups were established by X-ray diffraction, SEM, and TEM. Fourier Transform Infrared Spectroscopy was utilized to examine the data. It turns out to be a quick, environmentally friendly method that provides an economical and efficient way to synthesize AgNPs. The NPs produced in this study demonstrated the ability to germinate seeds, which may have applications in agriculture. In the near future, opto-electronics and medical devices will depend heavily on this environmentally benign method, which may be a competitive substitute for the conventional physical/chemical methods used to synthesize AgNPs. As a result, it may find usage in biomedical applications.

Acknowledgment

The authors wish to express their thanks to SSIP (Student Startup and Innovation Policy), Gandhinagar, Gujarat for providing a fund for this research work. The authors also wishes thanks to principal of Sheth M.N. Science College, Patan for providing a lab facility to explore this research work. Authors also acknowledge the SAIF, Chandigarh, Panjab University for FTIR, XRD, SEM and TEM analysis.

Reference

1. Panda K.K., Achary V.M., Krishnaveni R., *et al*. (2011). In vitro biosynthesis and genotoxicity bioassay of silver nanoparticles using plants. *Toxicol In Vitro*. ;25(5):1097-1105. https://doi.org/10.1016/j.tiv.2011.03.008

2. Sadowski, Zygmunt. (2010). Biosynthesis and Application of Silver and Gold Nanoparticles. https://doi.org/10.13140/2.1.2718.3042

3. Castro-Longoria, Ernestina & Vilchis-Nestor, Alfredo & Avalos-Borja, Miguel. (2010). Biosynthesis of silver, gold and bimetallic nanoparticles using the filamentous fungus *Neurospora crassa*. Colloids and surfaces. B, *Biointerfaces*. 83. 42-8. https://doi.org/10.1016/j.colsurfb.2010.10.035

4. Ahmed S., Saifullah, Mudasir Ahmad, Babu Lal Swami & Saiqa Ikram (2016). Green synthesis of silver nanoparticles using *Azadirachta indica* aqueous leaf extract, *Journal of Radiation Research and Applied Sciences*, 9:1, 1-7, 10.1016/j.jrras.2015.06.006

5. Bhattacharya R, Mukherjee P. (2008). Biological properties of "naked" metal nanoparticles. *Adv Drug Deliv Rev.* 60(11):1289-1306. https://doi.org/10.1016/j.addr.2008.03.013

6. Bhumkar, D.R., Joshi, H.M., Sastry, M. *et al*. Chitosan (2007). Reduced Gold Nanoparticles as Novel Carriers for Transmucosal Delivery of Insulin. *Pharm Res* 24, 1415–1426. https://doi.org/10.1007/s11095-007-9257-9

7. Azulai D., Belenkova T.,Gilon H., Barkay Z. And Markovich G., (2009). “Transparent metal nanowire thin films prepared in mesostructured templates,” *Nano letters*, 9, 12, pp.4246-4249 https://doi.org/10.1021/nl902458j

8. Sun Y., (2010). “Silver nanowires–unique templates for functional nanostructures,” *Nano scale*, Vol 2, pp.1626-1642, http://dx.doi.org/10.1039/C0NR00258E"

9. De S, Higgins TM, Lyons PE, *et al*. (2009). Silver Nanowire Networks as Flexible, Transparent, Conducting Films: Extremely High DC to Optical Conductivity Ratios. *ACS Nano*. 3(7):1767-1774. https://doi.org/10.1021/nn900348c

10. Jha, A., Prasad, K, Prasad, K, Kulkarni, AR (2009). "Plant system: nature's nanofactory". *Colloids Surf. Biointerfaces*, 73: p. 219-223.

11. Singh, S., Naresh, V., & Sharma, S. K. (2013). Isolation of novel phytoconstituents from the bark of *Salvadora oleoides* Decne. *International Journal of Herbal Medicine*, 1(2), 9–13.

12. Kumar, S., Dhankhar, S., Arya, V. P., Yadav, S., & Yadav, J. P. (2012). Antimicrobial activity of *Salvadora oleoides* Decne. against somemicroorganisms. *Journal of Medicinal Plant Research*, 6(14), 2754–2760.

13. Natubhai, P. M., Pandya, S. S., & Rabari, H. A. (2013). Anti inflammatory activity of leaf extracts of *Salvadora oleoides* Decne. *International Journal of Pharma and Biosciences*, 4(1), 985–993.

14. Simonsen, H. T. (2001). In vitro screening of Indian medicinal plants for antiplasmodial activity. *Journal of Ethnopharmacology*, 74,195–204.

15. Kathireswari, P. Gomathi S. and Saminathan K. (2014). Plant leaf mediated synthesis of silver nanoparticles using *Phyllanthus niruri* and its antimicrobial activity against multi drug resistant human pathogens, *Int.J.Curr.Microbiol.App.Sci*, 3(3) 960-968

16. Amudha M. and Krishna kumari S., (2014). In vitro: Phytochemical screening and evaluation of antioxidant potential of *Vitex negundo* Linn. Of synthesized silver nanoparticles, *wjpps*, volume 3, Issue 8, 1385-1393

17. Parvathalu, K., Chinmayee, S., Preethi, B. *et al.* Green Synthesis of Silver Nanoparticles Using *Argyreia nervosa* Leaf Extract and Their Antimicrobial Activity. *Plasmonics* **18**, 1075–1081 (2023). https://doi.org/10.1007/s11468-023-01835-8

18. Anandalakshmi K, Venugobal J (2017). Green Synthesis and Characterization of Silver Nanoparticles Using *Vitex negundo* (Karu Nochchi) Leaf Extract and its Antibacterial Activity. *Med Chem (Los Angeles)* 7: 218-225. https://doi.org/10.4172/2161-0444.1000460

19. Tripathy, A.; Raichur, A.M.; Chandrasekaran, N.; Prathna, T.; Mukherjee, A. (2010). Process variables in biomimetic synthesis of silver nanoparticles by aqueous extract of *Azadirachta indica* (Neem) leaves. *J. Nanopart. Res.* 12, 237–246. http://dx.doi.org/10.1007/s11051-009-9602-5

20. Saranayaadevi *et al*., (2014) Evaluation of Antioxidant Properties, Total Phenolic and Carotenoid Content of *Chaetoceros calcitrans*, *Chlorella salina* and *Isochrysis galbana*, *Int.J.Curr.Microbiol.App.Sci* 3(8) 365-377

21. Preetha Devaraj, Prachi Kumari, Chirom Aarti, Arun Renganathan (2013). "Synthesis and Characterization of Silver Nanoparticles Using *Cannonball Leaves* and Their Cytotoxic Activity against MCF-7 Cell Line", *Journal of Nanotechnology*, vol. 2013, Article ID 598328, 5 pages https://doi.org/10.1155/2013/598328

22. Allafchian, A.R., Mirahmadi-Zare, S.Z., Jalali, S.A.H. *et al*. (2016). Green synthesis of silver nanoparticles using *phlomis* leaf extract and investigation of their antibacterial activity. *J Nanostruct Chem* 6, 129–135 https://doi.org/10.1007/s40097-016-0187-0

23. GnanaDhas GnanaJobitha, Gurusamy Annadurai*1, Chellapandian Kannan*2 (2012). Green synthesis of Silver Nanoparticle using *Elettaria Cardamomom* and Assessment of its Antimicrobial Activity, *International Journal of Pharma Sciences and Research* (IJPSR) ISSN : 0975-9492 Vol 3 No 3

24. Shafaghat, A. (2014) Synthesis and Characterization of Silver Nanoparticles by Phytosynthesis Method and Their Biological Activity. *Synthesis and Reactivity in Inorganic, Metal-Organic, and Nano-Metal Chemistry*, 45, 381-387. http://dx.doi.org/10.1080/15533174.2013.819900

25. Ibrahim MFM, El-Gawad HG, Bondok AM. Physiological impacts of potassium citrate and folic acid on growth, yield and some viral diseases of plants. *Middle East J Agric Res*. 2015; 04:577-589.

26. Jung JH, Kim SW, Min JS, Kim YJ, Lamsal K, Kim KS *et al*. The effect of nano-silver liquid against the white rot of the green onion caused by Sclerotium cepivorum. Mycobiol. 2010; 38:39-45.